Laser and Particle Beams (2015), *33*, 713–722.

doi:10.1017/S026303461500083X

Generation of terahertz radiation by beating of two circular flat-topped laser beams in collisional plasma

FARHAD BAKHTIARI, MASOUD YOUSEFI, SHOLE GOLMOHAMMADY, SEYED MASOUD JAZAYERI, AND BIJAN GHAFARY

Physics Department, Iran University of Science and Technology, Heydarkhani, Tehran, Iran

(RECEIVED 26 April 2015; ACCEPTED 13 June 2015)

Abstract

This paper presents a scheme of terahertz (THz) radiation generation based on beating of two flat-topped laser beams by different frequencies and the same electric field amplitudes in actual plasma with spatially periodic density that electron–neutral collisions have been taken into account. Flat-topped laser beams have the exclusive features such as steep gradient in distribution of laser intensities, wider cross-section in comparison with other profiles, which make stronger ponderomotive force and lead to stronger nonlinear current and hence, THz radiation of higher field. The effects of laser and plasma parameters on THz radiation generation are investigated analytically. It is shown that by increasing the order of flatness of incident laser beams, because of their steep gradient, good enhancement in emitted THz radiation take place. It can be deduced that by increasing beating frequency, efficiency of THz generation decreases which can be compensated by manipulating in density ripple magnitudes. The intensity of the emitted radiations is found to be highly sensitive to the order of flatness. Based on the results of this paper, optimization of laser and plasma parameters can increase the efficiency of THz radiation generation strongly.

Keywords: Beating; collisional plasma; flat-topped laser beam; terahertz generation

1. INTRODUCTION

The terahertz, abbreviated THz, is a unit of electromagnetic wave frequency equal to 0.1–10 trillion hertz (10^{12} Hz) and is lying between infrared (IR) and microwave (MW) radiation in the electromagnetic spectrum. Like IR and MW radiation, THz radiation travels in a line of sight and is nonionizing. THz radiation, like MW radiation, can penetrate in a wide variety of non-conducting materials. The THz radiations attract surging interest in the field of spectroscopy, sub millimeter astronomy, manufacturing, quality control, process monitoring, chemical and material characterization, security screening, medical imaging, three-dimensional (3D) imaging of teeth, tomography, topography, communication, remote sensing, and so on (Beard *et al*., 2002; Ferguson & Zhang, 2002; Shen *et al*., 2005; Pickwell & Wallace, 2006; Zheng *et al*., 2006; Kleine-Ostmann & Nagatsuma, 2010; Akyildiz *et al*., 2014). A promising technology for generating and manipulating of THz radiation because of the lack of affordable, compact and high power THz sources is the subject and a great challenge for researchers (Singh & Sharma, 2013). Due to lack of efficient emitters and receptors, THz radiation had remained the last unexplored region. But during the last decade THz radiation, due to its varied applications, rapidly plays an important role in research. In consequence of relatively expensive and large THz sources, a lot of researches is being carried out for achieving suitable THz sources (Budiarto *et al*., 1996; Hashimshony *et al*., 2001; Shi *et al*., 2002; Tzortzakis *et al*., 2002; Holzman & Elezzabi, 2003; Sprangle *et al*., 2004; Liu *et al*., 2007; Houard *et al*., 2008; Jiang *et al*., 2011; Wang *et al*., 2011; Al-Naib *et al*., 2013). By applying electro-optic crystal (EO crystal), such as ZnSe, GaP, LiNbO3, or photo conductive antenna, super luminous laser–pulse interaction with large band gap semiconductors and dielectric, some generation schemes of THz sources have been introduced (Budiarto *et al*., 1996; Hashimshony *et al*., 2001; Shi *et al*., 2002; Holzman & Elezzabi, 2003; Jiang *et al*., 2011; Wang *et al*., 2011; Al-Naib *et al*., 2013). The researches show that the nonplasma based techniques (such as EO crystals and semiconductor) for THz emitters have the problem with high-power laser pulses because of material breakdown (Budiarto *et al*., 1996). Material breakdown in high-power laser pulses, low conversion

Address correspondence and reprint requests to: F. Bakhtiari, Physics Department, Iran University of Science and Technology, Heydarkhani, Tehran, Iran. E-mail: fbakhtiari@physics.iust.ac.ir

efficiency, and narrow bandwidth of emitted THz radiation are disadvantages of these types of THz sources. Due to these disadvantages, a lot of investigations have been done for introducing new schematic of THz generation. The plasma, being in an ionized state, can handle very high power, and hence, plasma-based schemes generally provide THz radiation with very high electric fields. The main challenge is to enhance the conversion efficiency of the generated THz radiation. In the consequence, interaction of highly intense ultra-short laser pulses in picosecond or femtosecond range with plasma has been proposed in various methods such as laser filamentation, cross-focusing, ponderomotive of laser pulse, and so on as a generation scheme of THz sources. Most of the THz generation mechanisms via laser filamentation are based on nonlinear forces like ponderomotive force. Due to the long-distance nature of the filament propagation, THz energy achieved from laser filaments is relatively high. Generation of THz radiation via filamentation process has been studied through several experimental and theoretical analyses and simulations (Tzortzakis *et al*., 2002; Sprangle *et al*., 2004; Liu *et al*., 2007; Houard *et al*., 2008; Bhasin & Tripathi, 2011). Many experiments employ plasma as a nonlinear medium for THz generation using sub picosecond laser pulses and energetic electron beams, since the plasma has the advantage that it can handle very high power and shows strong nonlinear effects (Pukhov, 2003; Leemans *et al*., 2004; Pathak *et al*., 2009; Zhang *et al*., 2012). THz amplification based on four-wave coupling in a plasma filled capillary, where two counter propagating laser pulses exert an electrostatic ponderomotive force on the electrons that drives longitudinal oscillations at beat frequency close to the plasma frequency, is investigated in detail (Yampolsky & Frainman, 2006).

Analytically investigation of the THz radiation generation by tunnel ionization of a gas jet by employing superposed field of femtosecond laser pulses impinging onto it after passing through an axicon has been done (Malik *et al*., 2010).

The effect of obliqueness of external magnetic field on the characteristics of magnetized plasma wake field, which can be used for the THz radiation generation, has been explored (Manouchehrizadeh & Dorranian, 2013; Hussain *et al*., 2014). Moreover, Laser beams with different intensity profiles behave differently in plasmas, and investigations have been made on THz generation by using diversified laser beam profiles, like Gaussian, super Gaussian, cosh-Gaussian, and triangular profiles with different plasma mediums (Bhasin & Tripathi, 2009; Malik *et al*., 2011*a*, *b*, 2012; Varshney *et al*., 2013, 2014*a*, *b*; Hussain *et al*., 2014; Singh & Malik, 2014; Singh & Sharma, 2014; Sharma & Singh, 2014; Jha & Verma, 2014; Bakhtiari *et al*., 2015; Kumar *et al*., 2015; Megesh Kumar *et al*., 2015). This work presents a model to produce THz radiation by using two flat-topped laser beams because of the exclusive features of flat-topped profile such as steep gradient in distribution of laser intensities, having wider cross-section into other profiles which make stronger ponderomotive force and lead to stronger nonlinear current and hence, THz radiation of higher field. In plasma medium, electron–neutral collisions have been taken into account. Since the collisions in actual plasma cannot be ignored, we solve the problem of phase matched THz radiation generation by ponderomotive force of two laser pulses.

This paper is organized as follows:

In Section 2, we introduce the flat-topped laser beams. We evaluate the efficiency and normalized emitted THz field strength with laser and plasma parameters such as laser beam width, order of flatness, plasma collision frequency, and density ripple magnitudes in Section 3. Section 4 presents the results and discussion of analytical investigations. Section 5 summarizes the conclusions.

2. FLAT-TOPPED LASER BEAM

A flat-top beam (or *top-hat beam*) is a laser beam having an intensity profile which is flat over most of the covered area. This is in contrast to Gaussian beams, for example, where the intensity smoothly decays from its maximum on the beam axis to zero. Such beam profiles are required for some laser applications. For example, nonlinear frequency conversion at very high power levels can be more efficient when performed with flat-topped beams.

The flat-topped laser beam has important applications in optical communication systems, some optical information processing techniques, material thermal processing, optical trapping, and electron acceleration (Kato *et al*., 1984; Nishi *et al*., 2000; Wang *et al*., 2006; Zhao *et al*., 2009; Golmohammady *et al*., 2013). Also, using the appropriate laser beam profile is one of the important methods for improving the efficiency of THz beam generation. Therefore, due to uniform cross-section profile, the flat-topped laser beam can be used in laser–plasma interaction field, especially in THz beam generation.

Several theoretical models, such as the super-Gaussian beam and flattened Gaussian beam have been proposed for describing a light beam with a flat-topped spatial profile (Perrone *et al*., 1993; Gori, 1994; Bagini *et al*., 1996; Cai & Lin, 2003). More recently, Li (2002*a*, *b*) proposed a new theoretical model to describe a flat-topped beam with circular or noncircular symmetries by expressing its field as a finite sum of fundamental Gaussian beams.

The generation of various flat-topped beams has been studied widely in the past 20 years (Kato *et al*., 1984; Perrone *et al*., 1993; Gori, 1994; Bagini *et al*., 1996; Borghi & Santarsiero, 1998; Nishi *et al*., 2000; Li, 2002*a*, *b*; Cai & Lin, 2003; Wang *et al*., 2006; Zhao *et al*., 2009; Golmohammady *et al*., 2013). In many cases, a flat-topped beam is obtained by first generating a Gaussian beam from a laser and then transforming its intensity profile with a suitable optical element such as lenses or mirrors having a cone-shaped surface. There are different kinds of beam shapers to do that transformation. For example, certain combinations of aspheric lenses

https://doi.org/10.1017/S026303461500083X Published online by Cambridge University Press

can be used, or some diffractive optics (Dickey *et al*., 2006; Chen *et al*., 2011; Forbes, 2013; Andrew, 2014). Also, recently a system containing two phase-only liquid crystal spatial light modulators is designed to convert a quasi-Gaussian beam into a flat-topped beam by Haotong *et al*. (2010).

In this work, we have proposed a mechanism of generating THz radiations using flat-topped laser beam as an incident beam in collisional plasma.

The electric field of a flat-topped laser beam with circular symmetry at the source plane, $z = 0$, can be expressed by Li (2002*a*, *b*):

$$\vec{E}_N(\vec{\rho}, \omega) = \sum_{n=1}^{N} E_{0\text{inc}} \frac{(-1)^{n-1}}{N} \binom{N}{n} \exp\left(-\frac{n\rho^2}{w_0^2}\right), \quad \vec{\rho} = (x, y) \quad (1)$$

Where $\vec{\rho}$ is transverse position vector. Also, N is the number of Gaussian beam sources which are assembled together to produce uniform profile and is called order of flatness and $\binom{N}{n}$ denotes a binomial coefficient. When $N = 1$, Eq. (1) reduces to a Gaussian beam evidently. The positive and independent of position coefficients $E_{0\text{inc}}$ and w_0 are the initial field amplitude and the effective beam width of the Gaussian beam, respectively.

By considering a constant electric field and the conservation of power in the different flatness order, the intensity distribution of flat-topped laser beam has been depicted in Figure 1. The covered area of uniform intensity of flat-topped laser beam is increased by increasing flatness order. By increasing order of flatness, the cross-section of flat-topped laser beam in incident plane of plasma enhances.

In the next section, THz radiation generation mechanism will be discussed in detail.

3. NONLINEAR CURRENT DUE TO LASER BEAM BEATING

Two circular flat-topped laser beams of frequencies ω_1 and ω_2 and wave numbers k_1 and k_2, respectively, with same electric field amplitude polarized along the y-direction, co-propagating in the z-direction, in a plasma that electron–neutral collisions with frequency of υ_{en} take place, are considered. The initial field distribution of the laser beams is given by:

$$\vec{E}_{Nj} = \left[\sum_{n=1}^{N} E_{0\text{inc}} \frac{(-1)^{n-1}}{N} \binom{N}{n} \exp\left(-\frac{ny^2}{w_{0y}^2}\right)\right] e^{i(k_j z - \omega_j t)} \hat{y}, \quad \text{with } j = 1, 2 \quad (2)$$

Laser beams beat together and impart a ponderomotive force to the plasma electrons at beat frequency $\omega = \omega_1 - \omega_2$ and wave number $k = k_1 - k_2$. Frequency difference of the lasers is in the THz range. The phase matching can be achieved by considering a plasma channel with a rippled modulated density together $n_e = n_{e0} + n'_\beta$, where $n'_\beta = n_\beta e^{ik_\beta z}$ and n_β and k_β are the amplitude and wave number of density ripples, such density ripples created by various techniques involving transmissive ring grating and a patterned mask where the control of ripple parameters might be possible by changing the groove period, groove structure, and duty cycle in such a grating and by adjusting the period and size of the masks (Hazra *et al*., 2004; Kuo *et al*., 2007; Layer *et al*., 2007; Kim *et al*., 2008; Bhasin & Tripathi, 2009; Malik *et al*., 2011*a*, *b*, 2012). Density ripples like an inhomogeneity couples with the density perturbations provided by ponderomotive force and give rise to nonlinear current responsible for THz generation. The force acting on electrons from lasers is expressed through the linearized equation of motion (Chen, 1983):

$$m_e \frac{d\vec{v}}{dt} = -e\vec{E}_{Nj} - m_e \upsilon_{en} \vec{v} \quad (3)$$

where collisional force $(-m_e \upsilon_{en} \vec{v})$ is taken into account. By solving the equation of motion, the velocity of electrons due to laser fields will be:

$$\vec{v}_j = \frac{e\vec{E}_{Nj}}{m_e(i\omega_j - \upsilon_{en})} \quad (4)$$

The lasers, due to gradient in their fields, also exert a nonlinear ponderomotive force to electrons which is dependent to electron velocities as (Boyd & Sanderson, 2003):

$$\vec{F}_p^{NL} = -\frac{m_e}{2} \nabla(\vec{v}_1 . \vec{v}_2^*) \quad (5)$$

In the presence of a nonlinear ponderomotive force, nonlinear perturbations of density of the electrons are governed by equation of continuity as:

$$n^{NL} = \frac{n_{e0}}{m_e i\omega(\upsilon_{en} - i\omega)} \nabla . \vec{F}_p^{NL} \quad (6)$$

By taking $\chi_e = -(\omega_p^2)/\omega(\omega + i\upsilon_{en})$ and $\omega_p^2 = 4\pi n_{e0} e^2/m_e$ as electric susceptibility and plasma frequency, respectively, nonlinear perturbations of density n^{NL} can be defined as:

$$n^{NL} = \frac{n_{e0}\chi_e}{m_e \omega_p^2} \nabla . \vec{F}_p^{NL} \quad (7)$$

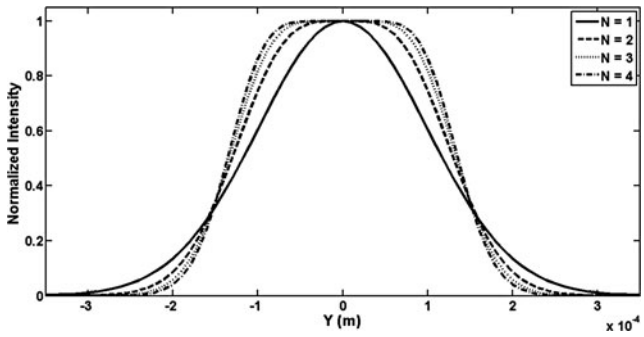

Fig. 1. Intensity diagram of modified flat top laser for different order of flatness ($N = 1$ corresponds to Gaussian beam).

https://doi.org/10.1017/S026303461500083X Published online by Cambridge University Press

In addition, linear density perturbation (n^{L}) is induced self-consistency by space charge field under influence of nonlinear perturbations in electron density, by producing a self-consistent space charge potential ϕ:

$$n^{\mathrm{L}} = -\frac{\chi_e \vec{\nabla}.(\vec{\nabla}\phi)}{4\pi e} \tag{8}$$

By using density perturbations, $\tilde{n} = n^{\mathrm{L}} + n^{\mathrm{NL}}$ the Poisson equation $\nabla^2\phi = 4\pi e\tilde{n}$, will be:

$$\begin{aligned}\vec{\nabla}.(\vec{\nabla}\phi) &= 4\pi e(n^{\mathrm{L}} + n^{\mathrm{NL}}) \\ &= 4\pi e\left(-\frac{\chi_e \vec{\nabla}.(\vec{\nabla}\phi)}{4\pi e} + \frac{n_{e0}\chi_e}{m_e\omega_p^2}\vec{\nabla}.\vec{F}_p^{\mathrm{NL}}\right)\end{aligned} \tag{9}$$

Hence, after sum simplifications, linear ponderomotive force obtains as nonlinear force:

$$\vec{F}^{\mathrm{L}} = e\vec{\nabla}\phi = \frac{\omega_p^2 \vec{F}_p^{\mathrm{NL}}}{i\omega(1+\chi_e)(\upsilon_{en} - i\omega)} \tag{10}$$

So the total electron velocity consist of linear force due to the self-consistent space-charge field and nonlinear ponderomotive force actions, can be obtained by again using equation of motion as $\partial\vec{v}^{\mathrm{NL}}/\partial t = \vec{F}^{\mathrm{L}}/m_e + (\vec{F}_p^{\mathrm{NL}}/m_e) - \upsilon_{en}\vec{v}$. So the resultant nonlinear electron velocity is achieved as:

$$\vec{v}_{\mathrm{T}}^{\mathrm{NL}} = \frac{i\omega\vec{F}_p^{\mathrm{NL}}}{m_e\left[i\omega(\upsilon_{en} - i\omega) - \omega_p^2\right]} \tag{11}$$

From this velocity, the nonlinear current density at ω, k' ($k' = k + k_\beta = k_1 - k_2 + k_\beta$) in the presence of the mentioned density ripple can be written as:

$$\begin{aligned}\vec{J}^{\mathrm{NL}} &= -\frac{1}{2}n'_\beta e\vec{v}^{\mathrm{NL}}{}_{\mathrm{T}} \\ &= -\frac{i\omega e n'_\beta}{2m_e\left[i\omega(\upsilon_{en} - i\omega) - \omega_p^2\right]}\vec{F}_p^{\mathrm{NL}}\end{aligned} \tag{12}$$

Since $\vec{J}^{\mathrm{NL}}$ is responsible for the generation of THz radiation.

4. CALCULATION OF EMITTED THZ FIELD

By letting Eq. (2) into Eq. (4) and the result in Eq. (5), then doing the mathematical derivative, the nonlinear ponderomotive force is realized as:

$$\begin{aligned}\vec{F}_p^{\mathrm{NL}} = &-\frac{e^2 {E_{0\mathrm{inc}}}^2}{2m_e(i\omega_1 - \upsilon_{en})(i\omega_2 + \upsilon_{en})} \\ &\times \sum_{m=1}^{M}\sum_{n=1}^{N}\frac{(-1)^{n+m-2}}{MN}\binom{N}{n}\binom{M}{m} \\ &\times \left[2\left(\frac{n+m}{w_{0y}}\right)\left(\frac{y}{w_{0y}}\right)\hat{y} - ik\hat{z}\right]e^{-(n+m)\left(\frac{y}{w_{0y}}\right)^2} e^{i(kz-\omega t)}\end{aligned} \tag{13}$$

Then by calculating nonlinear velocity from Eq. (11), the nonlinear oscillatory current density yields from Eq. (12) as:

$$\begin{aligned}\vec{J}^{\mathrm{NL}} = &\frac{1}{2}n'_\beta e\frac{e^2 {E_{0\mathrm{inc}}}^2}{m_e(i\omega_1 - \upsilon_{en})(i\omega_2 + \upsilon_{en})}\frac{i\omega}{m_e[\omega^2 - \omega_p^2 + i\omega\upsilon_{en}]} \\ &\times \sum_{m=1}^{M}\sum_{n=1}^{N}\frac{(-1)^{n+m-2}}{MN}\binom{N}{n}\binom{M}{m} \\ &\times \left[2\left(\frac{n+m}{w_{0y}}\right)\left(\frac{y}{w_{0y}}\right)\hat{y} - ik\hat{z}\right]e^{-(n+m)\left(\frac{y}{w_{0y}}\right)^2} e^{i(kz-\omega t)}\end{aligned} \tag{14}$$

Equation (14) shows that, the current density varies in accordance with $\vec{F}_p^{\mathrm{NL}} \sim \exp(i(kz - \omega t))$. After putting $n'_\beta = n_\beta e^{ik_\beta z}$ in Eq. (14), nonlinear current oscillates at the frequency ω but its wave number is $k' = k_1 - k_2 + k_\beta$. With the application of density ripples, the wave numbers can be tuned and resonant excitation of THz radiation can be realized (Malik *et al.*, 2012).

By using the Maxwell equations, the wave equation governing the propagation of THz wave can be written as:

$$\nabla^2\vec{E} - \nabla(\nabla.\vec{E}) + \frac{\omega^2}{c^2}(\varepsilon.\vec{E}) = \frac{-4\pi i\omega}{c^2}\vec{J}^{\mathrm{NL}} \tag{15}$$

where $\varepsilon = 1 + \chi_e = 1 - (\omega_p^2/\omega(\omega + i\upsilon_{en}))$ is the plasma permittivity at the THz frequency. Taking fast phase variations in $\vec{E}$ as $\vec{E} = \vec{E}_0(z)e^{i(k'z-\omega t)}$ the y-component of Eq. (15) that would be suitable for the THz emission can be deduced as:

$$2ik'\frac{dE_{0y}}{dz} + \left(\frac{\omega^2}{c^2}\varepsilon - k'^2\right)E_{0y} = \frac{-4\pi i\omega}{c^2}J_y^{\mathrm{NL}} \tag{16}$$

In the rippled density plasma, the exact phase matching condition demands that, $(\omega^2/c^2)\varepsilon - k'^2 = 0$, where $k' = k + k_\beta = k_1 - k_2 + k_\beta$, which can be obtained by placing the right-hand side of Eq. (16), source term, equal to zero. From this, vector k_β that is wave number of density ripples is given by:

$$\begin{aligned}k_\beta &= \frac{\omega}{c}Re\left[\left(1 - \frac{\omega_p^2}{\omega(\omega + i\upsilon_{en})}\right)^{1/2} - 1\right] \\ &= \frac{\omega}{c}\left[\left(1 - \frac{\omega_p^2}{\omega^2 + \upsilon_{en}^2}\right)^{1/2} - 1\right]\end{aligned} \tag{17}$$

Thus, the resonance condition coincides with $\omega \geq \sqrt{\omega_p^2 - \upsilon_{en}^2}$. The field is obtained only if the phase matching condition is met. In order to match the wave numbers of ponderomotive force and nonlinear current, density ripples with periodicity $2\pi/k_\beta$ are required to be constructed in the plasma. Hence, k_β represents wave number corresponding to density ripples.

https://doi.org/10.1017/S026303461500083X Published online by Cambridge University Press

Using phase matching condition in Eq. (16) and letting $d/dz \propto ik'$, will result to the following expression for the THz field $\vec{E}_{y\mathrm{THZ}} = (2\pi i/\omega\varepsilon)J_y^{\mathrm{NL}}$. By using Eq. (14) for the y component of J_y^{NL}, the normalized THz amplitude can be written as follows:

$$\left|\frac{E_{0\mathrm{THZ}}}{E_{0\mathrm{inc}}}\right| = \frac{\omega_\mathrm{p}^2 eE_{0\mathrm{inc}}\omega}{2m_\mathrm{e}}\left(\frac{n_\beta}{n_{\mathrm{e}0}}\right) \times \mathrm{real}\left[\frac{\omega + i\upsilon_{\mathrm{en}}}{(\omega_1 + i\upsilon_{\mathrm{en}})(\omega_2 - i\upsilon_{\mathrm{en}})\left(\omega^2 - \omega_\mathrm{p}^2 + i\omega\upsilon_{\mathrm{en}}\right)^2}\right] \times \sum_{m=1}^{M}\sum_{n=1}^{N}\frac{(-1)^{n+m-2}}{MN} \times \binom{N}{n}\binom{M}{m}\left[\left(\frac{n+m}{w_{0y}}\right)\left(\frac{y}{w_{0y}}\right)\right]e^{-(n+m)(y/w_{0y})^2} \tag{18}$$

Our concern is only on stationary solutions for THz radiation generation, thus Eq. (18) does not depend on the plasma length. For the parameters of present scheme, which will be defined, the THz radiation can easily propagate out of the plasma because damping of THz electro-magnetic wave is negligible and even plasma length can be adjusted in experimental set-ups according to the skin depth of plasma.

5. THZ RADIATION EFFICIENCY

The efficiency of the emitted radiation is the ratio of the energy of THz radiation and the energy of the incident lasers. According to Rothwell and Cloud (2009) the average electromagnetic energy stored per unit volume, in general, is given by the formula:

$$W_{\mathrm{Ei}} = \frac{\varepsilon}{8\pi}\frac{\partial}{\partial\omega_\mathrm{i}}\left[\omega_\mathrm{i}\left(1 - \frac{\omega_\mathrm{p}^2}{\omega_\mathrm{i}^2}\right)\right]\langle|E_\mathrm{i}|^2\rangle \tag{19}$$

Using this formula, the energy density of the lasers, that is, the energy per unit volume, is calculated as,

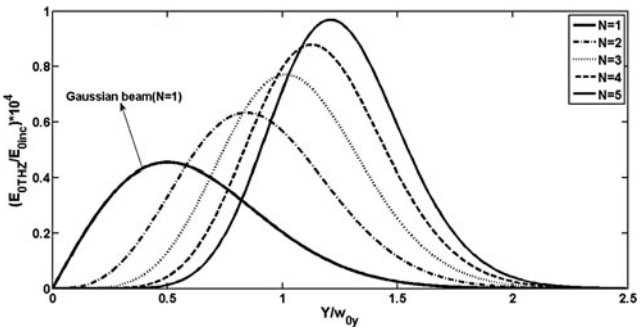

Fig. 2. Variation of normalized THz amplitude with normalized transverse distance in various order of flatness of incident lasers, when $\upsilon_{\mathrm{en}} = 0.05\omega_\mathrm{p}$ and $n_\beta/n_{\mathrm{e}0} = 0.3$. The case $N = 1$ corresponds to Gaussian beam.

$W_{\mathrm{LE}} = (\varepsilon/8\pi)(\partial/\partial\omega)[\omega(1 - \omega_\mathrm{p}^2/\omega)]\langle|E|^2\rangle$, while for the THz field is, $W_{\mathrm{THZ}} = (\varepsilon/8\pi)(\partial/\partial\omega)[\omega(1 - \omega_\mathrm{p}^2/\omega)]\langle|E_{\mathrm{THZ}}|^2\rangle$ after computing total average energy densities the efficiency of the THz radiation, η, following the methods used with Varshney *et al.* (2013); Varshney *et al.* (2014*a*, *b*); Singh and Malik (2014), by using Eq. (18) for $|E_{0\mathrm{THZ}}/E_{0\mathrm{inc}}|$, is obtained as follows:

$$\eta = \frac{W_{\mathrm{THZ}}}{W_{\mathrm{pump}}} = \left|\frac{E_{0\mathrm{THZ}}}{E_{0\mathrm{inc}}}\right|^2 = \left(\frac{\omega_\mathrm{p}^2 eE_{0\mathrm{inc}}\omega}{2m_\mathrm{e}}\left(\frac{n_\beta}{n_{\mathrm{e}0}}\right)\right)^2 \times \left(\frac{\omega^2 + \upsilon_{\mathrm{en}}^2}{\left(\omega_1^2 + \upsilon_{\mathrm{en}}^2\right)\left(\omega_2^2 + \upsilon_{\mathrm{en}}^2\right)\left(\left(\omega^2 - \omega_\mathrm{p}^2\right)^2 + \omega^2\upsilon_{\mathrm{en}}^2\right)^2}\right) \times \left[\sum_{m=1}^{M}\sum_{n=1}^{N}\frac{(-1)^{n+m-2}}{MN}\binom{N}{n}\binom{M}{m} \times \left[\left(\frac{n+m}{w_{0y}}\right)\left(\frac{y}{w_{0y}}\right)\right]e^{-(n+m)(y/w_{0y})^2}\right]^2 \tag{20}$$

6. RESULTS AND DISCUSSION

In what follows, we will compute field and efficiency of emitted THz radiation for various parameters of incident lasers such as beam width and order of flatness. Due to the importance of electron–neutral collisions in collisional plasma dynamic, effect of plasma parameters like collision frequency and amplitude of density ripples will be discussed in each case. The following set of parameters has been used in numerical calculations:

Laser initial field amplitude $E_{0\mathrm{inc}} = 2\times10^9$ V/m, initial beam waist width of laser beams $W_{0y} = 0.02$ cm, laser frequencies $\omega_1 = 2.4\times10^{14}$ rad/s and $\omega_2 = 2.1\times10^{14}$ rad/s are chosen which are corresponded to Pico-second CO_2 laser. Electron plasma frequency supposed as $\omega_\mathrm{p} = 2\times10^{13}$ rad/s which is corresponding to the electron plasma density $n_{\mathrm{e}0} = 1.25\times10^{23}$ m^{-3}. Density ripple amplitude is $n_\beta = 5.03\times10^{22}$ m^{-3} for $n_\beta/n_{\mathrm{e}0} = 0.4$.

In Figure 2, we examine the emitted radiation field amplitude with the normalized transverse distance (y/w_{0y}) for the different values of order of flatness of incident lasers. From which it is evident that by increasing the order of flatness of lasers, the magnitude of generated THz radiation increases in comparison with Gaussian laser beam. In the present scheme, the ponderomotive force plays an important role for generating nonlinear current that this effect is related to gradients of laser fields which is evident from Eq. (5). Increasing the order of flatness makes steep gradient in shape and distribution of laser intensities that is depicted in Figure 1. This steep gradient makes stronger ponderomotive force and leads to stronger nonlinear current and hence, THz radiation of higher field amplitude. By increasing the area of flatness, the occurrence of the field gradient moves outward

https://doi.org/10.1017/S026303461500083X Published online by Cambridge University Press

and causes that THz beam profile distance from the origin. In each order of flatness, THz field attain a maximum in a value of (y/w_{0y}) that is also altered. In this maximum point the ponderomotive force acquires maximum magnitude too. Place of these maximum peaks have been computed from the condition $d/dy(E_{0\mathrm{THZ}}/E_{0\mathrm{inc}}) = 0$ as:

$$\sum_{m=1}^{M}\sum_{n=1}^{N}\frac{(-1)^{n+m}}{MN}\binom{N}{n}\binom{M}{m} \times (n+m)\left[1-2(n+m)\left(\frac{y}{w_{0y}}\right)^2\right]e^{-(n+m)(y/w_{0y})^2} = 0 \quad (21)$$

For example for $N = 1$, 2, 3, 4, and 5, this maximum is $(y/w_{0y}) = 0.501$, 0.841, 1.011, 1.131, and 1.211 respectively, which is computed numerically. With the help of these points, one can focus the peak of radiation field at a desired position. Also all graphs show that by increasing the order of flatness, the emitted THz field profile has been quite symmetrical. The response of electron movement to applied field gradient strength because of varying shape of beam for their flatness is responsible for emitted beam shape. Intensity gradient of the lasers at the front and rear sides of the laser pulses, have opposite directions, and redound electron movement to be reversed. In small order of flatness, the electrons while moving back do not get enough response time to traverse their original path and hence, an asymmetry is introduced in their movement. However, with the increasing order of flatness and intensity gradient, the electrons by getting sufficient response time can make symmetry in their movements and hence, the emitted THz radiation profile being quite symmetrical. For this, THz field generated from Gaussian beam ($N = 1$) have minimum symmetry in its generated THz beam profile.

In Figure 3 effect of collision frequency on normalized emitted THz amplitude for different order of flatness and collision frequency, υ_{en}, is depicted. Increase in collisional frequency decreases generated field strength. Increasing the order of flatness can compensate the effect of collision. But it is evident that in the presence of larger collision frequency, the lasers with higher order of flatness are more affected and the field of THz radiation falls at faster rate in comparison with lower order of flatness and commonly Gaussian beam.

This effect also is depicted in Figure 4 separately, all orders of flatness attain a maximum for $\upsilon_{en} = 0$ (collisionless plasma) and it is shown that higher orders of flatness are more sensitive to increasing collision frequency and their field strength fall in faster rate.

Discussing role of amplitude of density ripples in THz radiation mechanism, variation of normalized emitted THz field amplitude with normalized density ripples is plotted in Figure 5. It can be concluded that, by increasing the magnitude of density ripples, the emitted field amplitude increases linearly which is also evident from Eq. (18). This effect is appreciable as more numbers of electrons take part in the oscillating current, which generates efficient THz radiation. Also higher order of flattens of laser beams, by making strength field gradients, upgrade field amplification. However, when collision frequency rises up, as excepted, the field strength decreases. For example, normalized emitted THz field amplitude of flatness $N = 2$ in low collision frequency, is quasi same as normalized emitted THz field amplitude of $N = 4$ in high collision frequency, in making amplification.

Also, there is an amazing point in this state. Because spatial part of emitted THz field in Eq. (18) does not depend on density ripple amplitude, by enhancing amplitude of density ripples, the emitted field strength increases, but the point which the maximum of field takes place is not changed. Also there is a fixed focus point for obtaining maximum field strength.

Due to the importance of the laser beam width on the THz radiation generation mechanism, in Figure 6, efficiency of emitted THz wave with beam width in different collision frequencies and order of flatness, have been plotted. The efficiency greatly reduces the larger beam width and a small change in beam width leads to the larger variation in the efficiency magnitude. Also collisional effects decrease the magnitude of efficiency and it can be seen from Figure 6 that by increasing collision in plasma, the rate of efficiency degrading decreases significantly. Moreover, by variation of beam width, the efficiency of generated THz from

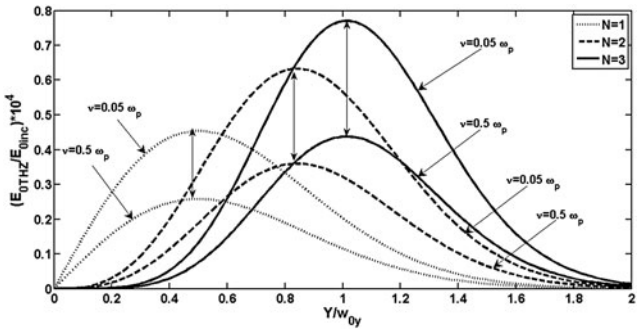

Fig. 3. Effect of collision frequency on normalized emitted THz amplitude in various order of flatness of incident lasers from $N = 1$ to 3 for two different values of collision frequency υ_{en}, when $n_\beta/n_{e0} = 0.3$.

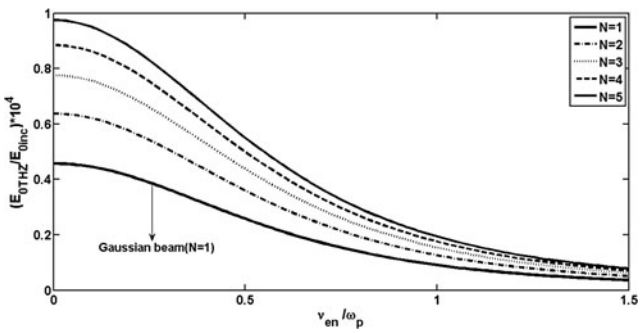

Fig. 4. Variation of normalized emitted THz amplitude with collision frequency for various order of flatness of incident lasers from $N = 1$ to 5 in their peak of maximum field in y/w_{0y} when $n_\beta/n_{e0} = 0.3$.

https://doi.org/10.1017/S026303461500083X Published online by Cambridge University Press

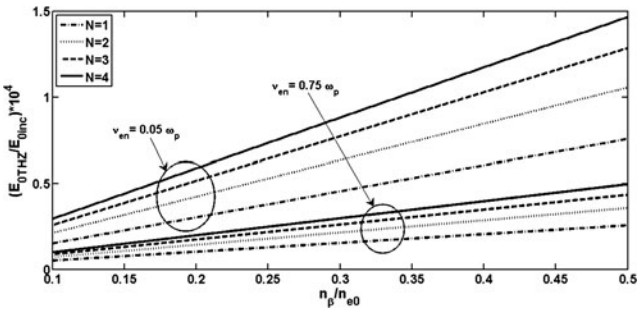

Fig. 5. Variation of normalized emitted THz amplitude with normalized density ripple amplitudes for various order of flatness of incident lasers from $N = 1$ to 4 in their peak of maximum field in y/w_{0y} for two different values of collision frequency.

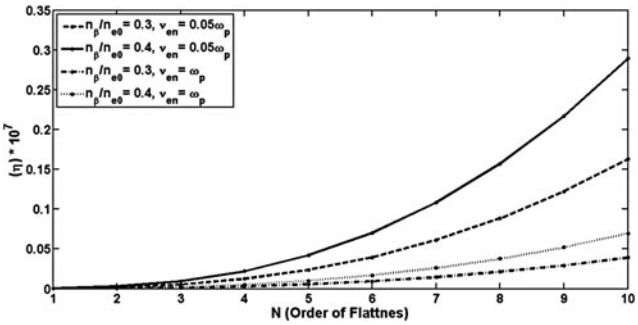

Fig. 7. Variation of efficiency of THz radiation with order of flatness of lasers (N) for different values of collision frequency and normalized density ripple amplitudes in their peak of maximum field in y/w_{0y}.

flat-topped and Gaussian laser beams have the same behavior, but in comparison with the results of the Singh and Malik (2014), which they had worked on THz generation with super Gaussian laser beams, it can be concluded that, the flat-topped laser beams is less sensitive to beam width variations.

By increasing the order of flatness of laser beams, efficiency of THz radiation enhances and this fact is very much affected by collision frequency, which is presented in Figure 7. Moreover by increasing the magnitude of density ripples in plasma, efficiency of THz radiation generation can enhance, which is evident from Figure 7. Also, there is an important point that in small degree of plasma density ripples, increasing order of flatness of laser would not enhance the efficiency effectively. The rate of efficiency enhancing is much related to magnitude of density ripples.

Figures 2–7 show that lasers with higher flatness order, produce stronger THz radiation along with higher efficiency of the mechanism and can be a good substitute for Gaussian lasers in THz generation using plasma. Also collisions have decreasing effect and density ripples amplitudes have additive effects in efficiency, and higher order of flattens are more sensitive to collision.

In this scheme, the condition of resonant excitation of THz radiation is that the Eq. (17) being established hence, as said before, density ripples with periodicity $2\pi/k_\beta$ are required to be constructed in the plasma. Hence $k_\beta c/\omega_p$ represents normalized wave number corresponding to density ripples. By using Eq. (17), dependency of normalized wave number of periodic structure of the density ripples with normalized beat wave frequency for different values of the collision frequency is depicted in Figure 8.

When collision frequency is very low, by increasing the normalized beat wave frequency, the normalized period of the rippled density structure decreases, but in high values of the collision frequency it increases slightly. For conquering the effect of collision and having a best exact phase matching, by increasing the normalized beat wave frequency, the normalized period of the rippled density structure must be increased. For the study of this effect in our scheme, Figure 9 shows the efficiency of THz radiation generation with normalized beating frequency for different values of normalized ripple amplitudes. By increasing normalized beating frequency, the efficiency decreases and one can compensate this effect by increasing density ripple amplitudes. It is evident that a higher efficiency is achieved when higher amplitude density ripples are employed. Also, collision has decreasing effect on efficiency as normalized beating frequency increases which is in accordance with the result of phase matching condition.

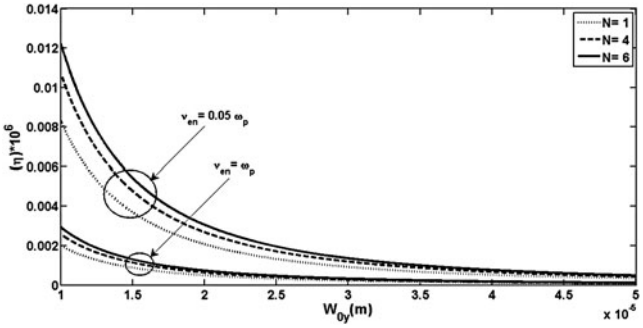

Fig. 6. Variation of efficiency of emitted THz radiation with beam width w_{0y} for different values of order of flatness and collision frequency in their peak of maximum field in y/w_{0y} and $n_\beta/n_{e0} = 0.3$.

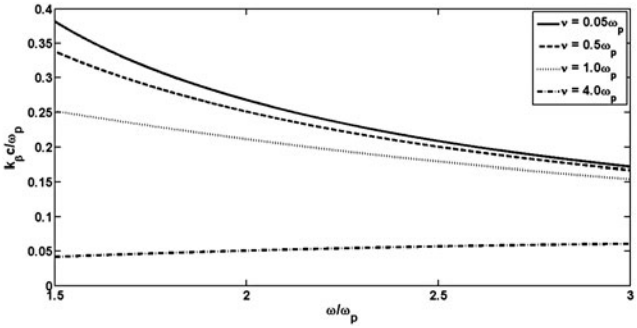

Fig. 8. Variation of normalized wave number of periodic structure of the density ripples with normalized beat wave frequency for different values of the collision frequency.

https://doi.org/10.1017/S026303461500083X Published online by Cambridge University Press

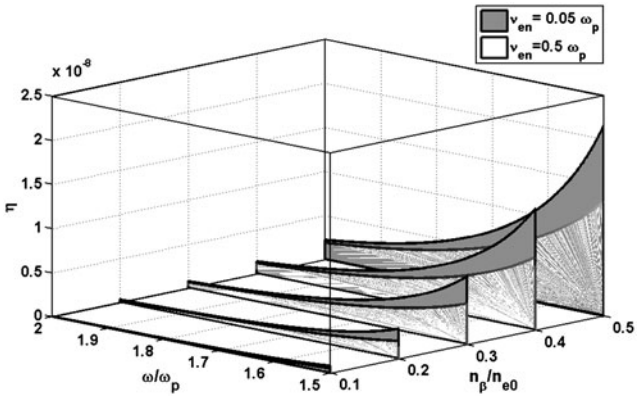

Fig. 9. *3D* plot of variation of efficiency of THz radiation generation with normalized beating frequency from the *z*-axis and normalized density ripple amplitudes for different values of collision frequency when $N = 4$ and $y = 1.125w_{0y}$.

7. CONCLUSIONS

In our analytical model, THz radiation generation mechanism by beating of two circular flat-topped laser beams in the collisional plasma with a rippled modulated density has been discussed. Effects of laser and plasma parameters in THz generation mechanism such as electron–neutral collisions, order of flatness, laser beam widths, beating frequency, and so on, is examined. It can be deduced that:

(1) By producing a flat-topped laser beam, we would have an intensity distribution in a big cross-section in incident plane of laser–plasma interaction, hence a strength field gradient will be produced, and that is very applicable for enhancing generation of THz radiation. We can say that by using the rectangular laser beams (by increasing order of flatness) because of their beam shapes, very strong THz radiation can be achieved and can be a good substitute for Gaussian lasers in THz generation using plasma.
(2) By increasing the order of flatness of incident laser beams, the emitted field profile is quite symmetrical and in each order of flatness, there is a focus point for emitted field.
(3) When collision frequency increases in plasma, the efficiency of THz radiation decreases significantly and the scheme is more sensitive to collision by increasing the order of flatness.
(4) The efficiency of THz decreases by increasing beating frequency, and it is very dependent to collision frequency.
(5) Amplitude of density ripples has additive effect on THz radiation field. By increasing the beat frequency which must be accompanied by increasing the period of the rippled density structure, best efficiency enhancement and phase matching can be achieved.
(6) Similar observations for the effect of intensity gradient of rectangular beam shape lasers in THz radiation generation mechanism are made by Singh and Malik (2014) and Malik *et al*. (2012) for THz generation with Super-Gaussian laser beams. In many cases, a flat-topped laser beam is obtained by first generating a Gaussian beam from a laser and then transforming its intensity profile with a suitable optical element such as lenses or mirrors having a cone-shaped surface which have been used out of laser cavity. But a super-Gaussian beam produces with resonance modes inter laser cavity such as digital micro-mirror devices (Van *et al*., 1994; Dickey *et al*., 2006; Forbes, 2013; Xiang *et al*., 2015) and for this reason, this laser beam production have complex technology in comparison with flat-topped beam production. Also, since mathematical form of flat-topped beam is closer to reality it can better introduce rectangular beam properties. Furthermore, due to important applications of flat-topped laser beam in optical communication systems, some optical information processing techniques, material thermal processing, optical trapping, and electron acceleration makes it disposable for THz generation applications.

Finally by balancing between orders of flatness, beam width of incident laser beams and density ripple amplitude, it can be achieved to a focus point with a good efficiency in exit plane of plasma and conquer to the effect of collision in plasma.

ACKNOWLEDGEMENT

This work has been done with the scientific support of Photonics laboratory, Department of Physics, Iran University of Science and Technology. The authors thank members of Photonics lab for supporting the research project. The authors appreciate Dr. Mahdi Esmaeilzadeh and Dr. Fatemeh D.Kashani for their consultation.

REFERENCES

Akyildiz, I.F., Jornet, J.M. & Han, Ch. (2014). Terahertz band: Next frontier for wireless communications. *Phys. Commun. (Elsevier)* **12**, 16–32.

Al-Naib, I., Sharma, G., Dignam, M., Hafez, H., Ibrahim, A., Cooke, D.G., Ozaki, T. & Morandotti, R. (2013). Effect of local field enhancement on the nonlinear terahertz response of a silicon-based metamaterial. *Phys. Rev. B* **88**, 195203-1–195203-8.

Andrew, F. (2014). *Laser Beam Propagation: Generation and Propagation of Customized Light*. Boca Raton: CRC Press, Taylor & Francis Group.

Bagini, V., Borgi, R., Gori, F., Pacileo, A.M. & Santarsiero, M.J. (1996). Propagation of axially symmetric flattened Gaussian beams. *Opt. Soc. Am. A* **13**, 1385–1394.

Bakhtiari, F., Golmohammady, Sh., Yousefi, M., Kashani, F.D. & Ghafary, B. (2015). Generation of terahertz radiation in collisional plasma by beating of two dark hollow laser beams. *Laser Part. Beams* **33**, 463–472.

https://doi.org/10.1017/S026303461500083X Published online by Cambridge University Press

Beard, M.C., Turner, G.M. & Schmuttenmar, C.A. (2002). Measuring intra-molecular charge transfer via coherent generation of THz radiation. *J. Phys. Chem. B* **106**, 7146–7159.

Bhasin, L. & Tripathi, V.K. (2009). Terahertz generation via optical rectification of x-mode laser in a rippled density magnetized plasma. *Phys. Plasma* **16**, 103105.

Bhasin, L. & Tripathi, V.K. (2011). Terahertz generation from laser filaments in the presence of a static electric field in a plasma. *Phys. Plasmas* **18**, 123106/1-4.

Borghi, R. & Santarsiero, M. (1998). Modal decomposition of partially coherent flat-topped beams produced by multimode lasers. *Opt. Lett.* **23**, 313–315.

Boyd, T.J.M. & Sanderson, J.J. (2003). *The Physics of Plasmas*. New York: Cambridge University Press.

Budiarto, E., Margolies, J., Jeong, S., Son, J. & Bokor, J. (1996). High-intensity terahertz pulses at 1-kHz repetition rate. *IEEE J. Quantum Electron.* **32**, 1839–1846.

Cai, Y. & Lin, Q. (2003). Properties of a flattened Gaussian beam in the fractional Fourier transform plane. *J. Opt. A: Pure Appl. Opt.* **5**, 272–275.

Chen, F.F. (1983). *Introduction to Plasma Physics and Controlled Fusion*. New York: Plenum Press.

Chen, J., Yu, Y. & Wang, F. (2011). Production of annular flat-topped vortex beams. *Chin. Opt. Lett.* **9**, 011402/1–4.

Dickey, F.M., Holswade, S.C. & Shealy, D.L. (2006). *Laser Beam Shaping Applications*. New York: CRC Press.

Ferguson, B. & Zhang, X.C. (2002). Materials for terahertz science and technology. *Nat. Mater.* **1**, 26–33.

Forbes, A. (2013). *Laser Beam Propagation*. Pretoria, South Africa: CRC Press.

Golmohammady, S.H., Yousefi, M., Kashani, F.D. & Ghafary, B. (2013). Reliability analysis of the flat-topped array beam FSO communication link. *J. Mod. Opt.* **60**, 696–703.

Gori, F. (1994). Flattened Gaussian beams. *Opt. Commun.* **107**, 335–341.

Haotong, M., Zejin, L., Zhou, P., Wang, X., Yanxing, M. & Xiaojun, X. (2010). Generation of flat-top beam with phase-only liquid crystal spatial light modulators. *J. Opt.* **12**, 045704.

Hashimshony, D., Zigler, A. & Papadopoulos, K. (2001). Conversion of electrostatic to electromagnetic waves by superluminous ionization fronts. *Phys. Rev. Lett.* **86**, 2806–2809.

Hazra, S., Chini, T.K., Sanyal, M.K. & Grenzer, J. (2004). Ripple structure of crystalline layers in ion-beam-induced Si wafers. *Phys. Rev. B* **70**, 121307(R).

Holzman, J.F. & Elezzabi, A.Y. (2003). Two-photon photoconductive terahertz generation in ZnSe. *Appl. Phys. Lett.* **83**, 2967–2969.

Houard, A., Liu, Y., Prade, B., Tikhonchuk, V.T. & Mysyrowicz, A. (2008). Strong enhancement of terahertz radiation from laser filaments in air by a static electric field. *Phys. Rev. Lett.* **100**, 255006.

Hussain, S., Singh, M., Singh, R.K. & Sharma, R.P. (2014). THz generation by self-focusing of hollow Gaussian laser beam in magnetized plasma. *Europhys. Lett.* **107**, 65002-p1–65002-p6.

Jiang, Y., Li, D., Ding, Y.J. & Zotova, I.B. (2011). Terahertz generation based on parametric conversion: from saturation of conversion efficiency to back conversion. *Opt. Lett.* **36**, 1608–1610.

Jha, P. & Verma, N.K. (2014). Numerical and simulation study of terahertz radiation generation by laser pulses propagating in the extraordinary mode in magnetized plasma. *Phys. Plasmas* **21**, 063106/1–6.

Kato, Y., Mima, K., Miyanaga, N., Arinaga, S., Kitagawa, Y., Nakatsuka, M. & Yamanaka, C. (1984). Random phasing of high power lasers for uniform target acceleration and plasma-instability suppression. *Phys. Rev. Lett.* **53**, 1057–1060.

Kim, K.Y., Taylor, A.J., Glownia, J.H. & Rodriguez, G. (2008). Coherent control of terahertz supercontinuum generation in ultrafast laser-gas interactions. *Nat. Photonics* **2**, 605.

Kleine-Ostmann, T. & Nagatsuma, T. (2010). A review on terahertz communications research. *J. Infrared Milli. Terahz. Waves* **32**, 143–171.

Kumar, S., Singh, R.K., Singh, M. & Sharma, R.P. (2015). THz radiation by amplitude-modulated self-focused Gaussian laser beam in ripple density plasma. *Laser Part. Beams* **33**, 257–263.

Kuo, C.C., Pai, C.H., Lin, M.W., Lee, K.H., Lin, J.Y., Wang, J. & Chen, S.Y. (2007). Enhancement of relativistic harmonic generation by an optically preformed periodic plasma waveguide. *Phys. Rev. Lett.* **98**, 033901.

Layer, B.D., York, A., Antonson, T.M., Varma, S., Chen, Y.H., Leng, Y. & Milchberg, H.M. (2007). Ultrahigh-intensity optical slow-wave structure. *Phys. Rev. Lett.* **99**, 035001-1–035001-4.

Leemans, W.P., Vantilborg, J., Faure, J., Geddes, C.G.R., Toth, C., Schroeder, C.B., Esarey, E., Fubioni, G. & Dugan, G. (2004). Terahertz radiation from laser accelerated electron bunches. *Phys. Plasmas* **11**, 2899.

Li, Y. (2002). Light beam with flat-topped profiles. *Opt. Lett.* **27**, 1007–1009.

Li, Y. (2002). New expressions for flat-topped light beams. *Opt. Commun.* **206**, 225–34.

Liu, Y., Houard, A., Prade, B., Akturk, S. & Mysyrowicz, A. (2007). Terahertz radiation source in air based on bifilamentation of femtosecond laser pulses. *Phys. Rev. Lett.* **99**, 135002.

Malik, A.K., Malik, H.K. & Kawata, S. (2010). Investigations on terahertz radiation generated by two superposed femtosecond laser pulses. *J. Appl. Phys* **107**, 113105.

Malik, A.K., Malik, H.K. & Nishida, Y. (2011*a*). Tunable terahertz radiation from a tunnel ionized magnetized plasma cylinder. *Phys. Lett. A* **375**, 1191.

Malik, A.K., Malik, H.K. & Stroth, U. (2011*b*). Strong terahertz radiation by beating of spatial-triangular lasers in a plasma. *Appl. Phys. Lett.* **99**, 071107.

Malik, A.K., Malik, H.K. & Stroth, U. (2012). Terahertz radiation generation by beating of two spatial-Gaussian lasers in the presence of a static magnetic field. *Phys. Rev. E* **85**, 016401-1–016401-9.

Manouchehrizadeh, M. & Dorranian, D. (2013). Effect of obliqueness of external magnetic field on the characteristics of magnetized plasma wake field. *J. Theor. Appl. Phys.* **7**, 43–48.

Magesh Kumar, K.K., Kumar, M., Yuan, T., Sheng, Z.M. & Chen, M. (2015). Terahertz radiation from plasma filament generated by two-color laser gas–plasma interaction. *Laser Part. Beams* **33**, 473–479.

Nishi, N., Jitsuno, T., Tsubakimoto, K., Matsuoka, S., Miyanaga, N. & Nakatsuka, M. (2000). Two-dimensional multi-lens array with circular aperture spherical lens for flat-top irradiation of inertial confinement fusion target. *Opt. Rev.* **7**, 216–220.

Pathak, V.B., Dahiya, D. & Tripathi, V.K. (2009). Coherent terahertz radiation from interaction of electron beam with rippled density plasma. *J. Appl. Phys.* **105**, 013315/1-5.

Perrone, M. R., Piegari, A. & Scaglione, S. (1993). On the super-Gaussian unstable resonators for high-gain short pulse laser media. *IEEE J. Quantum Elec.* **29**, 1423–1427.

https://doi.org/10.1017/S026303461500083X Published online by Cambridge University Press

Pickwell, E. & Wallace, V.P. (2006). Biomedical applications of terahertz technology. *J. Phys. D: Appl. Phys.* **39**, R301–R310.

Pukhov, A. (2003). Strong field interaction of laser radiation. *Rep. Prog. Phys.* **66**, 47.

Rothwell, E.J. & Cloud, M.J. (2009). *Electromagnetic*. Boca Raton: CRC Press, Taylor and Francis Group.

Sharma, R.P. & Singh, R.K. (2014). Terahertz generation by two cross focused laser beams in collisional plasmas. *Phys. Plasma* **21**, 073101-1–073101-6.

Shen, Y.C., Lo, T., Taday, P.F., Cole, B.E., Tribe, W.R. & Kemp, M.C. (2005). Detection and identification of explosives using terahertz pulsed spectroscopic imaging. *Appl. Phys. Lett.* **86**, 241116-1–241116-3.

Shi, W., Ding, Y.J., Fernelius, N. & Vodopyanov, K. (2002). Efficient, tunable, and coherent 0.18–5.27-THz source based on GaSe crystal. *Opt. Lett.* **27**, 1454–1456.

Singh, D. & Malik, H.K. (2014). Terahertz generation by mixing of two super-Gaussian laser beams in collisional Plasma. *Phys. Plasmas* **21**, 083105-1–083105-5.

Singh, M. & Sharma, R.P. (2013). Generation of THz radiation by laser plasma interaction. *Contrib. Plasma Phys.* **53**, 540–548.

Singh, R.K. & Sharma, R.P. (2014). Terahertz generation by two cross focused Gaussian laser beams in magnetized plasma. *Phys. Plasma* **21**, 113109-1–113109-6.

Sprangle, P., Penano, J. R., Hafizi, B. & Kapetanakos, C.A. (2004). Ultrashort laser pulses and electromagnetic pulse generation in air and on dielectric surfaces. *Phys. Rev. E* **69**, 066415.

Tzortzakis, S., Mechhain, G., Patalano, G., Andre, Y.B., Prade, B., Franco, M., Mysyrowicz, A.M., Munier, J.M., Gheudin, M., Beaudin, G. & Encrenaz, P. (2002). Coherent subterahertz radiation from femtosecond infrared filaments in air. *Opt. Lett.* **27**, 1944–1946.

Van, N.R., Park, C., Lachance, L.R. & Bklanger, P.A. (1994). Graded-Phase mirror resonator with a Super-Gaussian output in a CW-CO_2 laser. *IEEE J. Quantum Electron.* **30**, 2663–2669.

Varshney, P., Sajal, V., Baliyan, S., Sharma, N.K., Chauhan, P., Kumar, R. (2014*a*). Strong terahertz radiation generation by beating of two x-mode spatial triangular lasers in magnetized plasma. *Laser Part. Beams* **33**, 51–58.

Varshney, P., Sajal, V., Chauhan, P., Kumar, R. & Sharma, N.K. (2014*b*). Effects of transverse static electric field on terahertz radiation generation by beating of two transversely modulated Gaussian laser beams in a plasma. *Laser Part. Beams* **32**, 375–381.

Varshney, P., Sajal, V., Singh, K.P., Kumar, R. & Sharma, N.K. (2013). Strong terahertz radiation generation by beating of extra-ordinary mode lasers in a rippled density magnetized plasma. *Laser Part. Beams* **31**, 337–344.

Wang, W., Wang, P.X., Ho, Y.K., Kong, Q., Chen, Z., Gu, Y., & Wang, S.J. (2006). Field description and electron acceleration of focused flattened Gaussian laser beams. *Europhys. Lett.* **73**, 211–217.

Wang, W.M., Kawata, S., Sheng, Z.M., Li, T.Y. & Zhang, J. (2011). Towards gigawatt terahertz emission by few-cycle laser pulses. *Phys. Plasmas* **18**, 073108-1–073108-6.

Xiang, Y.D., Yu, X.R. & Rong, D.L. (2015). Shaping super-Gaussian beam through digital micro-mirror device. *Sci. China – Phys. Mech. Astron.* **58**, 1–6.

Yampolsky, N.A. & Frainman, G.M. (2006). Conversion of laser radiation to terahertz frequency waves in plasma. *Phys. Plasmas* **13**, 113108.

Zhang, Y.X., Zhou, Y.C., Dong, L. & Liu, S.G. (2012). Coherent terahertz radiation from high-harmonic component of modulated free-electron beam in a tapered two-asymmetric grating structure. *J. Appl. Phys.* **101**, 123503/1-4.

Zhao, C., Cai, Y., Lu, X., & Eyyuboglu, H.T. (2009). Radiation force of coherent and partially coherent flat-topped beams on a Rayleigh particle. *Opt. Express* **17**, 1753–1765.

Zheng, H., Redo-Sanchez, A. & Zhang, X.C. (2006). Identification and classification of chemicals using terahertz reflective spectroscopic focal-plane imaging system. *Opt. Express* **14**, 9130–9141.